JOURNAL OF GEOPHYSICAL RESEARCH, VOL. 100, NO. C7, PAGES 13,321–13,332, JULY 15, 1995

Variability in the chlorophyll-specific absorption coefficients of natural phytoplankton: Analysis and parameterization

Annick Bricaud, Marcel Babin, André Morel, and Hervé Claustre

Laboratoire de Physique et Chimie Marines, CNRS and
Université Pierre et Marie Curie, Villefranche-sur-Mer, France

Abstract. Variability in the chlorophyll (chl) *a*-specific absorption coefficients of living phytoplankton $a^*_{ph}(\lambda)$ was analyzed using a data set including 815 spectra determined with the wet filter technique in different regions of the world ocean (covering the chlorophyll concentration range 0.02–25 mg m^{-3}). The a^*_{ph} values were observed to decrease rather regularly from oligotrophic to eutrophic waters, spanning over more than 1 order of magnitude (0.18 to 0.01 m^2 mg^{-1}) at the blue absorption maximum. The observed covariation between $a^*_{ph}(\lambda)$ and the field chl *a* concentration ⟨chl⟩ can be explained considering (1) the level of pigment packaging and (2) the contribution of accessory pigments to absorption. Empirical relationships between $a^*_{ph}(\lambda)$ and ⟨chl⟩ were derived by least squares fitting to power functions. These relationships can be used to produce a^*_{ph} spectra as a function of ⟨chl⟩. Such a simple parameterization, if confirmed with further data, can be used, e.g., for refining estimates of the carbon fixation rate at global or regional scales, such as those obtained by combining satellite pigment concentration maps with primary production models based on physiological parameters, among which a^*_{ph} is an important one.

1. Introduction

In oceanic waters, optical properties of phytoplankton, and specifically their in vivo absorption coefficients, play a key role in determining both the penetration of the radiant energy within seawater and the use of this radiant energy for photosynthesis. Spectral light absorption and backscattering are the two inherent optical properties directly ruling the diffuse reflectance R of the ocean, and thus ocean color, through a relationship of the form:

$$R(\lambda) = F b_b(\lambda)/a(\lambda)$$

where a and b_b are, respectively, the absorption and backscattering coefficients of the water body, and the dimensionless number F depends, in particular, on the volume scattering function within water [*Prieur and Morel*, 1975] and on the geometrical structure of the incident light field [*Kirk*, 1984; *Gordon*, 1989; *Morel and Gentili*, 1991].

Analytical models of the phytoplankton growth and primary production also basically rely on the in vivo absorption capacity of living algal cells [*Kiefer and Mitchell*, 1983; *Platt and Sathyendranath*, 1988; *Morel*, 1991; *Anderson*, 1993], namely, on the absorption coefficients of phytoplankton per unit of chlorophyll (chl) *a* concentration ("chl *a*-specific" coefficients or, equivalently, absorption cross sections of algae per mass unit of chl *a*, hereafter denoted $a^*_{ph}(\lambda)$ and expressed as m^2 mg chl a^{-1}). Such models, combined with satellite data, have been recently used to convert maps of surface pigment concentration into maps of the carbon fixation rate at global or regional scales [e.g., *Morel and André*, 1991]. Up until now, in the application of these models (with the exception of that of *Platt and Sathyendranath* [1988]), $a^*_{ph}(\lambda)$ coefficients have been assumed as constant, whatever the water type, and values considered as "typical" have been introduced.

These coefficients, however, are now widely recognized as varying, not only for individual species grown in culture, but also for natural phytoplanktonic assemblages [e.g., *Mitchell and Kiefer*, 1988b; *Bricaud and Stramski*, 1990]. These variations result from the combined influences of the pigment composition [*Bidigare et al.*, 1990; *Hoepffner and Sathyendranath*, 1992] and the so-called "package effect" [*Kirk*, 1975]. The latter, as predicted by theory, describes the variations of $a^*_{ph}(\lambda)$ for pigmented particles as a function of a parameter combining cell size and absorption coefficient of the cellular matter [*Morel and Bricaud*, 1981].

In the natural environment, how these different causes of variation cumulate or compensate their effects on $a^*_{ph}(\lambda)$ is presently not well known. Various field studies [*Mitchell and Kiefer*, 1988b; *Yentsch and Phinney*, 1989; *Bricaud and Stramski*, 1990; *Mitchell and Holm-Hansen*, 1991; *Babin et al.*, 1993] have substantiated variations in $a^*_{ph}(\lambda)$, due either to taxonomic changes within the algal crop (with correlative changes in both cell size and intracellular pigment concentration) or to photoadaptation within the local population (inducing changes only in the intracellular pigment concentration, as a response to variations in light intensity).

Several authors have investigated the relationship between the chl *a*-specific absorption coefficients of phytoplankton at selected wavelengths and the chl *a* concentration within the water body, hereafter denoted ⟨chl⟩ and expressed as milligrams per cubic meter. A first, indirect approach to this problem was proposed by *Prieur and Sathyendranath* [1981], who derived the total absorption coefficients from diffuse attenuation spectra measured in various waters. From a classification of these spectra according to their shape, they proposed a power law in $\langle chl \rangle^{0.6}$ to express the variations (at 440 nm) of the absorption coefficient of phyto-

Paper number 95JC00463.
0148-0227/95/95JC-00463$05.00

plankton. This coefficient, however, included the phytoplankton derivatives and by-products with similar optical effects. *Yentsch and Phinney* [1989] carried out direct absorption measurements (using the "filter technique" [*Trüper and Yentsch*, 1967]) in waters of the western North Atlantic, ranging from the oligotrophic waters of the Sargasso Sea to the eutrophic waters of the Gulf of Maine. They observed nonlinear relationships between the chlorophyll-specific particulate absorption coefficients, $a_p^*(440)$ and $a_p^*(670)$, and $\langle chl \rangle$ and attributed the variations in a_p^* to differences in nutrient availability and correlatively in cell size (inducing a variable package effect). Their study, however, did not discriminate between algal and nonalgal (detrital) absorptions, so that the measured coefficients are not directly comparable to the a_{ph}^* coefficients to be specifically studied here.

Bricaud and Stramski [1990] determined absorption coefficients of living phytoplankton (separately from detrital absorption) and found a_{ph}^* values systematically higher in the Sargasso Sea than in mesotrophic waters off Peru. They interpreted this difference as resulting mainly from the package effect, as only a small part was accounted for by variations in the pigment composition. *Wozniak and Ostrowska* [1990], who gathered a large set of a_{ph}^* spectral data in various regions, observed a distinct increase of a_{ph}^* throughout the blue-green wavelength domain with decreasing $\langle chl \rangle$ levels. They attributed this trend solely to the increasing contribution of accessory pigments, with no consideration of the package effect. They established statistical relationships between $a_{ph}^*(\lambda)$ and a "pigment index," thereafter introduced in a light-photosynthesis model [*Wozniak et al.*, 1992]. For their measurements made with the filter technique, however, no precise information is given on the correction of the path length amplification "β" factor, which is crucial when trying to derive accurate values of particle absorption [*Mitchell and Kiefer*, 1988a; *Bricaud and Stramski*, 1990].

In view of taking into account the variability of a_{ph}^* in a reflectance model, *Carder et al.* [1991] recently proposed hyperbolic tangent expressions to represent a_{ph}^* (at three different wavelengths) as a function of $\langle chl \rangle$, with different numerical coefficients for subtropical and temperate regions. These expressions, however, relying on very few experimental results, were proposed only tentatively. *Babin et al.* [1995] also observed an overall decrease of $a_{ph}^*(435)$ as a function of $\langle chl \rangle$ for the Gulf of St. Lawrence waters. In contrast, *Hoepffner and Sathyendranath* [1992] did not find, for the Gulf of Maine and Georges Bank regions (and over a $\langle chl \rangle$ range 0.05–2.5 mg m^{-3}), any dependency of $a_{ph}^*(440)$ on $\langle chl \rangle$.

With regard to the increasing use of analytical reflectance and light-photosynthesis models in the interpretation of remote sensing data, it seems timely to reinvestigate more systematically the relationship between $a_{ph}^*(\lambda)$ and $\langle chl \rangle$ for different trophic situations and to examine whether such a relationship, if any, is ubiquitous or site dependent. While it is acknowledged that $a_{ph}^*(\lambda)$ is affected by different factors, such as the package effect and pigment composition, a possible correlative change of both these factors with the trophic status of waters may contribute to the existence of a link between the $a_{ph}^*(\lambda)$ and $\langle chl \rangle$ evolutions. The aim of this paper is thus to investigate the existence of such a relationship; even if approximate, it should allow an improved parameterization of $a_{ph}^*(\lambda)$ to be introduced in models used to estimate primary production from ocean color data.

Note that the present approach is not to be confounded with the one used by *Smith and Baker* [1978] and *Morel* [1988]. These authors have studied the diffuse attenuation coefficients for downwelling irradiance $K_d(\lambda)$ and introduced $\langle chl \rangle$-dependent expressions derived from statistical analyses. These coefficients, once divided by $\langle chl \rangle$, provide "chlorophyll-specific diffuse attenuation coefficients" (often referred to as "k_c" coefficients), also $\langle chl \rangle$ dependent (see, e.g., [*Morel*, 1988, Figure 10a]). These k_c coefficients differ from a_{ph}^*, as they merge the contributions of living phytoplankton and of other associate particles to absorption and scattering (which act simultaneously in forming K_d); they also include the contribution of covarying dissolved matter to absorption. $\langle chl \rangle$ dependency of k_c was attributed by these authors mainly to a regular variation in the relative proportions of algal and nonalgal components with changing standing crop, without particular attention paid to the possibility of a variation in the a_{ph}^* coefficient.

2. Data and Methods

To examine the relationship between $a_{ph}^*(\lambda)$ and $\langle chl \rangle$, a data set including 815 samples was built up by gathering the results of several oceanographic cruises in various regions of the world ocean (see Table 1). For all samples, absorption spectra of total particulate matter collected on 25-mm Whatman GF/F filters, $a_p(\lambda)$, were measured with adapted spectrophotometers ("wet filter technique" [*Trüper and Yentsch*, 1967]). For most of the cruises, absorption spectra of nonalgal (mainly detrital) material $a_d(\lambda)$ were also experimentally determined using the chemical (extractive) method of *Kishino et al.* [1985]. Then the absorption spectra of living phytoplankton $a_{ph}(\lambda)$ were obtained by subtracting $a_d(\lambda)$ from $a_p(\lambda)$. For some of the cruises (Paciprod, Lidar 89, and Lidar 90), $a_d(\lambda)$ was not measured but derived using a numerical decomposition method based on spectral criteria. Detailed procedures have been described by *Bricaud and Stramski* [1990], who also showed that the a_{ph} spectra provided by both methods are in excellent agreement when applied to the same sample. All a_{ph} spectra were corrected for the path length amplification effect by using the algorithm given by *Bricaud and Stramski* [1990]. Chl *a*-specific absorption coefficients of phytoplankton $a_{ph}^*(\lambda)$ were finally obtained by dividing $a_{ph}(\lambda)$ (m^{-1}) by the chl *a* concentration (milligrams per cubic meter), including divinyl (div) chl *a*, if any.

Pigment concentrations were determined using various techniques (high-pressure liquid chromatography (HPLC), broadband fluorometry, spectrofluorometry, or spectrophotometry; see Table 1). HPLC determinations of liposoluble pigments were made as described by *Claustre and Marty* [1995]. Fluorometric determinations of chlorophylls and pheopigments were carried out using the method of *Yentsch and Menzel* [1963] for the Lidar 89 cruise and the modified method of *Holm-Hansen and Riemann* [1978] for the Paciprod cruise. Spectrofluorometric determinations of chlorophylls and pheopigments were made according to *Neveux and Lantoine* [1993]. Finally, spectrophotometric measurements were made according to the method described by *Parsons et al.* [1984].

A comparison between simultaneous spectrofluorometric

Table 1. Information Concerning the Cruises Where Absorption Data Were Collected

Cruise	Location	Period	Dominant Water Type	⟨Chl⟩ Range, mg m^{-3}	Sampling Depths, m	Pigment Measurements	a_d Measurements	N	Reference
Paciprod	Peru upwelling	Aug.–Sept. 1986	M	0.5–1.8	0–75	fluorometry	···	30	1, 4
Chlomax	Sargasso Sea	Sept.–Oct. 1987	O	0.03–0.33	0–180	spectrofluorometry	x	52	1, 5
Lidar 89	St. Lawrence estuary and Gulf	September 1989	E, M	0.8–24.5	1.5–9.5	fluorometry	···	249	2
Lidar 90	St. Lawrence estuary and Gulf	July 1990	E, M	0.16–8.3	2–25	spectrophotometry	···	239	2, 3
Tomofront	Liguro-Provençal Basin	April 1990	M	0.15–1.8	5–170	HPLC	x	29	
Mediprod 6	SW Mediterranean	July 1990	E, M	0.06–7.5	0–100	spectrofluorometry	x	67	6
Eumeli 3	tropical North Atlantic	Oct. 1991	M, O	0.017–1.9	0–150	HPLC (and spectrofluorometry)	x	124	
Eumeli 4	tropical North Atlantic	June 1992	E, M, O	0.05–4.8	10–170	HPLC	x	25	

The dominant water type is indicated by E, M, or O for eutrophic, mesotrophic, and oligotrophic waters, respectively. HPLC is high-pressure liquid chromatography. The a_d measurements (cross symbols) indicate that detrital absorption spectra have been experimentally determined using the method of *Kishino et al.* [1985]. N is the number of samples for each cruise. References are 1, *Bricaud and Stramski* [1990]; 2, *Babin et al.* [1993]; 3, *Babin et al.* [1995]; and 4, 5, 6 cruise reports from *Groupe MEDIPROD* [1989, 1992, 1991], respectively.

and HPLC determinations on more than 200 samples during the Eumeli 3 cruise has shown that the (chl *a* plus divchl *a*) concentrations measured by both methods were very well correlated. Spectrofluorometric values, however, were steadily higher than HPLC values, by 21%, on average, at the mesotrophic site and 33% at the oligotrophic site, mostly due to differing estimates of divchl *a* concentrations. In order to ensure the consistency of the data set, the HPLC method was chosen as the reference method, and spectrofluorometric values were converted accordingly, using a site-dependent "correction" factor. No correction was applied to spectrophotometric values, as divchl *a* pigments can be assumed to be in negligible quantity in the (mostly eutrophic) area where this method was used. Finally, fluorometric determinations, made with a broadband detector, are also believed to be only weakly influenced by the variable proportion of divchl *a* and were not corrected.

For all samples, pheophytin *a* was included in the (chl *a* plus divchl *a*) concentration. Except for deep waters and some eutrophic waters, the relative concentration of pheophytin *a* was in most cases no more than a few percent of the total concentration. The few absorption spectra unambiguously influenced by pheopigments and identified by an anomalously high absorption around 420 nm (using the simple criterion $a^*_{ph}(420) > a^*_{ph}(440)$) were eliminated from the data set.

3. Results

The variations of $a^*_{ph}(\lambda)$ as a function of ⟨chl⟩ are shown in Figure 1 at four wavelengths (412, 443, 490, and 565 nm) selected so as to correspond to the blue and green channels of the future sea-viewing wide field-of-view sensor (SeaWiFS) color sensor and at a fifth wavelength (675 nm) corresponding to the red absorption band of chl *a*. In spite of some visible scatter (discussed later), $a^*_{ph}(\lambda)$ shows a clear trend to decrease with increasing ⟨chl⟩, at 412, 443, and 490 nm and, less markedly, at 675 nm. The $a^*_{ph}(443)$ values, for instance, decreases by more than 1 order of magnitude (0.18 to 0.01 m^2 mg^{-1}) when ⟨chl⟩ varies from 0.02 to 25 mg m^{-3}. This trend almost completely vanishes at 565 nm. Furthermore, at this wavelength a few points stand apart from the main cluster, due to an exceptionally high phycoerythrin content in the corresponding samples from the tropical North Atlantic (see examples in Figure 2).

At the wavelengths where $a^*_{ph}(\lambda)$ is noticeably varying the decrease of a^*_{ph} with increasing ⟨chl⟩ can be represented by various mathematical expressions (see appendix for a discussion of the validity of this approach). The power function

$$a^*_{ph}(\lambda) = A(\lambda)\langle \text{chl} \rangle^{-B(\lambda)} \quad (1)$$

where A and B are positive, wavelength-dependent parameters, appears to be the most appropriate, i.e., providing the highest determination coefficient. Least squares fits to (1) were therefore performed between 400 and 700 nm, with a 2-nm step.

The spectral values of the exponent B, along with the determination coefficients on the log-transformed data r^2 are shown in Figure 3; the $A(\lambda)$ values are shown in Figure 7, as the $a^*_{ph}(\lambda)$ spectrum corresponding to ⟨chl⟩ = 1 mg m^{-3}. All these values are listed in Table 2. The spectral values of the exponent B exhibit a pattern similar to an absorption spectrum, except that the blue maximum is shifted from ~440 to 480 nm. This means that the deformation of the a^*_{ph} spectrum with changing ⟨chl⟩ is most accentuated within the absorption bands, particularly those of accessory pigments. $B(\lambda)$ values exceed 0.3 around the blue absorption maximum (430–500 nm), while they drop to ~0.16 at the red absorption maximum and are essentially 0 in the green part of the spectrum, where a^*_{ph} is no longer correlated to ⟨chl⟩.

In spite of the visible dispersion in the a^*_{ph} versus ⟨chl⟩ relationship (Figure 1), r^2 values remain higher than 0.7 throughout the blue domain (400–500 nm). Consistently with $B(\lambda)$, $r^2(\lambda)$ exhibits a maximum around 470–480 nm, while it

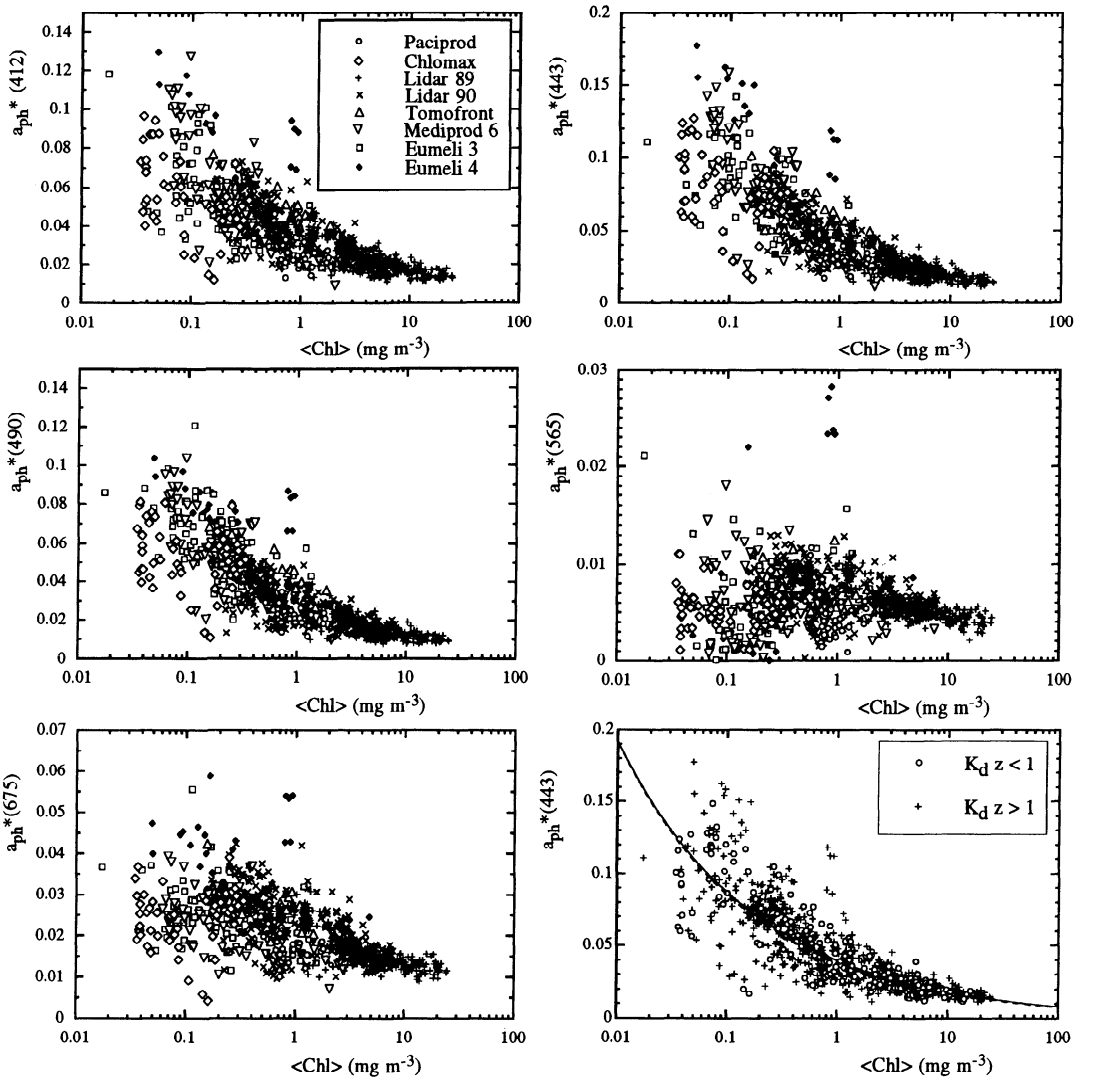

Figure 1. Variations of the chlorophyll-specific absorption coefficients of living phytoplankton $a^*_{ph}(\lambda)$ (in square meters per milligram), as functions of the (chl *a* + divinyl chl *a*) concentration ⟨chl⟩ (in milligrams per cubic meter), at selected wavelengths and for various regions of the world ocean (see Table 1). In the bottom right panel the samples have been sorted into those located within the first optical depth ($K_d z < 1$) and the deeper samples ($K_d z > 1$). The (practically undistinguishable) regression curves corresponding to all samples and to surface samples only are shown as a solid line and as a dashed line, respectively.

falls down to 0.3–0.4 around the red absorption band of chl *a* and to ~0 in the green part of the spectrum, where *B* is also close to 0.

It was suggested by *Carder et al.* [1991] that the ⟨chl⟩ dependency of a^*_{ph} could differ between regions. In our data set, however, such differences between regions cannot be discerned from the intrasite variability. Therefore all data were pooled together, and unique couples of *A* and *B* values were derived for each wavelength. It is acknowledged, however, that many marine systems are not represented in our data set, especially those which are known to have differing bio-optical properties, such as low-light, high-nutrient Antarctic waters [*Mitchell and Holm-Hansen*, 1991].

As samples from LIDAR cruises are numerically dominant in the data set (488 out of 815 samples), it could be suspected that *A* and *B* values have been biased by the inclusion of these samples. It has been checked that this is actually not the case. At 443 nm, for instance, *A* varies from 0.0394 to 0.0406 and *B* varies from 0.344 to 0.330, according to whether or not these 488 samples are included in the analysis. The main effect of including these samples is to increase the determination coefficient (from 0.49 to 0.77 at 443 nm), without altering the best fit curve.

The observed relationships between $a^*_{ph}(\lambda)$ and ⟨chl⟩ merge at least two different types of covariations: covariations from site to site and covariations along the vertical at a given site. To discriminate between these two types of covariation, $a^*_{ph}(443)$ values were split into the following two categories: (1) one including "surface samples," defined as being located within the first optical depth, and (2) another one including samples collected at larger depths. The first optical depth was simply computed as $z_e/4.6$, where z_e, the euphotic depth, was estimated for each station, either di-

rectly from the measured downwelling photosynthetically available radiation (PAR) irradiance profile when available or indirectly from the pigment vertical profile [*Morel*, 1988]. When fitting the variations of $a^*_{ph}(443)$ versus ⟨chl⟩ to a power law for surface samples only, the regression curve is practically confounded with that obtained when all samples are pooled together (Figure 1, bottom right panel). Therefore both site-to-site and vertical covariations of a^*_{ph} and ⟨chl⟩ follow similar trends, which allows these scales to be merged in the analysis of a^*_{ph} variations.

4. Discussion

The general trend of the a^*_{ph} values to increase with decreasing ⟨chl⟩, most accentuated in the blue part of the spectrum (Figure 1), could be suspected to originate from an artifact. As the relative contribution of detrital matter to total absorption tends to increase with decreasing ⟨chl⟩ (see, e.g., *Bricaud and Stramski* [1990, Figure 18]), imperfectly eliminated detrital absorption could lead to an artificial increase of a^*_{ph} at low ⟨chl⟩. When examining the variations of $a_{ph}(440)$ as a function of ⟨chl⟩, however, no intercept at null ⟨chl⟩ can be discerned (Figure 4). This suggests that a_{ph} does not include any significant contribution of absorbing detrital matter. It is also clear from Figure 4 that $a_{ph}(440)$ does not vary linearly as a function of ⟨chl⟩ but exhibits a curvature well represented by a power law, as actually used (see (1)).

The drawback inherent to a power law for representing the a^*_{ph} versus ⟨chl⟩ relationship is that it cannot provide realistic upper and lower bounds to a^*_{ph}, as, for instance, the hyperbolic tangent function chosen by *Carder et al.* [1991] does. The applicability of (1) is obviously limited to the ⟨chl⟩ range covered by the data set, namely, 0.02–25 mg m^{-3}.

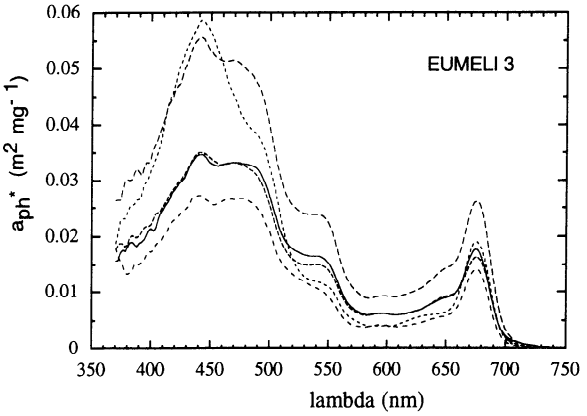

Figure 2. Examples of chlorophyll-specific absorption spectra $a^*_{ph}(\lambda)$ (in square meters per milligram), as determined at the mesotrophic site during the Eumeli 3 cruise. Note that the absorption shoulder due to phycoerythrin, as visible around 550 nm, in principle, cannot be observed on a^*_{ph} spectra obtained with *Kishino et al.*'s [1985] method. Usually, phycobilins are not removed by methanol extraction and, consequently, are (erroneously) included in the detrital compartment. In our particular procedure, however [see *Bricaud and Stramski*, 1990], the bleached filter is soaked again in seawater before detrital absorption measurements, so that water-soluble pigments are allowed to be, at least partly, extracted.

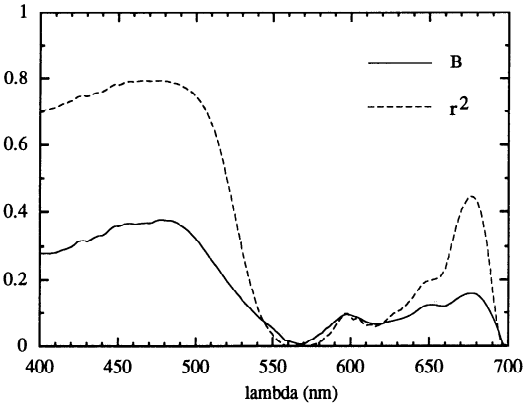

Figure 3. Spectral values of the exponents B of the power laws representing the variations of $a^*_{ph}(\lambda)$, as functions of the (chl a + divchl a) concentration (see equation (1)), and of the determination coefficients on the log-transformed data r^2. No smoothing has been applied to these spectra. The values are tabulated in Table 2.

Nevertheless, this range is wide enough to encompass most of the chlorophyll concentrations expected in the world ocean.

The decrease of $a^*_{ph}(\lambda)$ with increasing ⟨chl⟩, as observed in this study, is thought to have two main causes as follows: (1) an increasing package effect from oligotrophic to eutrophic waters [e.g., *Yentsch and Phinney*, 1989] and (2) a possible inverse covariation between the relative abundance of accessory pigments (chl b, chl c, and carotenoids) and the ⟨chl⟩ level. The respective effects of these two processes are examined below.

4.1. The Package Effect

The package effect can be quantified as the ratio of a^*_{ph}, the specific absorption coefficient of pigmented cells, to a^*_{sol}, the specific absorption coefficient of the same cellular matter ideally dispersed into solution. This dimensionless factor, denoted Q^*_a, has been theoretically formulated as follows [*Morel and Bricaud*, 1981]:

$$Q^*_a = (3/2)Q_a(\rho')/\rho' \tag{2}$$

where Q_a, the mean efficiency factor for absorption by phytoplanktonic cells, is a function of the parameter ρ' [*van de Hulst*, 1957]

$$Q_a = 1 + 2[\exp(-\rho')/\rho'] + 2\{[\exp(-\rho') - 1]/\rho'^2\} \tag{3}$$

and ρ' is the product of the absorption coefficient of the cellular matter a_{cm} and the cell size d,

$$\rho' = a_{cm}d \tag{4}$$

According to (2) and (3), Q^*_a continuously decreases from 1 (no package effect) to 0 (maximal package effect) with increasing ρ' values [see *Morel and Bricaud* [1981, Figure 1]). Since, at most wavelengths, a_{cm} is influenced by the pigment composition (and not only by the presence of chl a), the importance of the package effect cannot be, in general, assessed independently from the variations in this pigment composition. A minimal influence of accessory pigments, however, is to be expected within the red absorption band of chl a (675 nm), except for the possible presence of chl b or

Table 2. Spectral Values of the Constants Obtained When Fitting the Variations of $a^*_{ph}(\lambda)$ Versus the (chl *a* + divchl *a*) Concentration ⟨Chl⟩ to Power Laws of the Form $a^*_{ph}(\lambda) = A(\lambda)\ \langle \text{Chl} \rangle^{-B(\lambda)}$ and Determination Coefficients on the Log-Transformed Data r^2

λ, nm	*A*	*B*	r^2	λ, nm	*A*	*B*	r^2
400	0.0263	0.282	0.702	402	0.0271	0.281	0.702
404	0.0280	0.282	0.706	406	0.0290	0.281	0.707
408	0.0301	0.282	0.710	410	0.0313	0.283	0.713
412	0.0323	0.286	0.718	414	0.0333	0.291	0.723
416	0.0342	0.293	0.725	418	0.0349	0.296	0.729
420	0.0356	0.299	0.733	422	0.0359	0.306	0.739
424	0.0362	0.313	0.746	426	0.0369	0.316	0.747
428	0.0376	0.317	0.749	430	0.0386	0.314	0.746
432	0.0391	0.318	0.750	434	0.0395	0.324	0.754
436	0.0399	0.328	0.757	438	0.0401	0.332	0.761
440	0.0403	0.332	0.762	442	0.0398	0.339	0.767
444	0.0390	0.348	0.774	446	0.0383	0.355	0.779
448	0.0375	0.360	0.783	450	0.0371	0.359	0.781
452	0.0365	0.362	0.783	454	0.0358	0.366	0.788
456	0.0354	0.367	0.789	458	0.0351	0.368	0.791
460	0.0350	0.365	0.789	462	0.0347	0.366	0.791
464	0.0343	0.368	0.792	466	0.0339	0.369	0.793
468	0.0335	0.369	0.793	470	0.0332	0.368	0.792
472	0.0325	0.371	0.792	474	0.0318	0.375	0.793
476	0.0312	0.378	0.793	478	0.0306	0.379	0.793
480	0.0301	0.377	0.791	482	0.0296	0.377	0.790
484	0.0290	0.376	0.788	486	0.0285	0.373	0.786
488	0.0279	0.369	0.783	490	0.0274	0.361	0.779
492	0.0267	0.356	0.774	494	0.0258	0.349	0.770
496	0.0249	0.341	0.763	498	0.0240	0.332	0.756
500	0.0230	0.321	0.747	502	0.0220	0.311	0.735
504	0.0209	0.300	0.722	506	0.0199	0.288	0.706
508	0.0189	0.275	0.686	510	0.0180	0.260	0.664
512	0.0171	0.249	0.641	514	0.0163	0.237	0.615
516	0.0156	0.224	0.578	518	0.0149	0.211	0.541
520	0.0143	0.196	0.498	522	0.0137	0.184	0.459
524	0.0131	0.173	0.417	526	0.0126	0.162	0.374
528	0.0121	0.151	0.332	530	0.0117	0.139	0.287
532	0.0113	0.129	0.248	534	0.0108	0.119	0.211
536	0.0104	0.109	0.176	538	0.0100	0.100	0.147
540	0.0097	0.090	0.116	542	0.0093	0.081	0.092
544	0.0090	0.073	0.074	546	0.0086	0.066	0.057
548	0.0083	0.059	0.044	550	0.0080	0.052	0.033
552	0.0076	0.044	0.023	554	0.0072	0.036	0.014
556	0.0068	0.027	0.007	558	0.0065	0.016	0.002
560	0.0062	0.016	0.002	562	0.0059	0.013	0.001
564	0.0057	0.010	0.001	566	0.0055	0.007	0.000
568	0.0054	0.007	0.000	570	0.0053	0.005	0.000
572	0.0053	0.011	0.001	574	0.0052	0.018	0.003
576	0.0052	0.022	0.004	578	0.0052	0.028	0.007
580	0.0053	0.035	0.013	582	0.0054	0.040	0.016
584	0.0055	0.050	0.028	586	0.0055	0.056	0.033
588	0.0056	0.065	0.043	590	0.0056	0.073	0.058
592	0.0057	0.081	0.072	594	0.0056	0.088	0.084
596	0.0056	0.093	0.097	598	0.0055	0.095	0.098
600	0.0054	0.092	0.086	602	0.0054	0.088	0.078
604	0.0055	0.086	0.083	606	0.0055	0.082	0.078
608	0.0056	0.076	0.067	610	0.0057	0.071	0.060
612	0.0059	0.069	0.063	614	0.0060	0.066	0.062
616	0.0062	0.063	0.056	618	0.0063	0.064	0.061
620	0.0065	0.064	0.063	622	0.0066	0.068	0.073
624	0.0067	0.071	0.083	626	0.0068	0.074	0.092
628	0.0069	0.076	0.099	630	0.0071	0.078	0.104
632	0.0073	0.080	0.109	634	0.0074	0.084	0.119
636	0.0075	0.088	0.128	638	0.0076	0.093	0.138
640	0.0077	0.098	0.149	642	0.0078	0.105	0.164
644	0.0079	0.113	0.177	646	0.0080	0.119	0.189
648	0.0081	0.123	0.195	650	0.0083	0.124	0.197
652	0.0085	0.125	0.200	654	0.0089	0.124	0.203
656	0.0095	0.122	0.206	658	0.0104	0.120	0.218
660	0.0115	0.121	0.235	662	0.0129	0.125	0.269
664	0.0144	0.131	0.308	666	0.0161	0.137	0.345
668	0.0176	0.143	0.377	670	0.0189	0.149	0.404
672	0.0197	0.153	0.424	674	0.0201	0.157	0.439
675	0.0201	0.158	0.445	676	0.0200	0.159	0.445

Table 2. (continued)

λ, nm	A	B	r^2	λ, nm	A	B	r^2
678	0.0193	0.158	0.444	680	0.0182	0.155	0.433
682	0.0166	0.148	0.406	684	0.0145	0.138	0.368
686	0.0124	0.124	0.315	688	0.0102	0.107	0.247
690	0.0083	0.086	0.164	692	0.0067	0.065	0.094
694	0.0054	0.042	0.036	696	0.0044	0.015	0.004
698	0.0036	−0.016	0.003	700	0.0030	−0.034	0.012

The λ is wavelength; A and B are numerical constants.

divinyl chl b. When corrected for the enhancement due to the presence of these pigments (by measuring the height of the band above a baseline joining $a^*_{ph}(660)$ to $a^*_{ph}(700)$), in vivo absorption at 675 nm is mostly due to chl a. Therefore, with the specific absorption coefficient of chl a in solution taken equal to 0.0207 m^2 mg chl a^{-1} at 675 nm [*Bricaud et al.*, 1983], the variations of $Q^*_a(675)$ can be assessed as $a^*_{ph}(675)/0.0207$ and examined as a function of ⟨chl⟩ (Figure 5).

Over the ⟨chl⟩ range, $Q^*_a(675)$ decreases approximately from 1 (the theoretical maximum value) to less than 0.3. Superimposed on this clear trend, there appears noticeable scatter, which is believed to be partly due to the uncertainty in the pathlength amplification β factor. This uncertainty increases with decreasing optical density [*Mitchell and Kiefer*, 1988a; *Bricaud and Stramski*, 1990] and therefore is much higher in the red part of the spectrum than in the blue part. This uncertainty is also presumably at the origin of $Q^*_a(675)$ values exceeding their theoretical upper limit, 1.

The package effect appears therefore to increase, on average, from oligotrophic to eutrophic waters, with a threefold decrease of $Q^*_a(675)$ over the experienced ⟨chl⟩ range. This result suggests that there would exist a covariation between ⟨chl⟩ and the product $(a_{cm}d)$, or equivalently, the product (c_id), where c_i, the intracellular chl a concentration, is equal to $a_{cm}(675)/0.0207$. This assumption is bolstered by two arguments. The first one is related to the site-to-site change in dominant species: several authors [e.g., *Herbland et al.*, 1985; *Carder et al.*, 1986] have observed a correlation between average cell size d and nutrient availability, which, in turn, suggests a correlation between d and the trophic situation, as depicted by ⟨chl⟩ [*Carder et al.*, 1991]. Even if such a correlation may fail in some areas (such as in high-nutrient, low-biomass waters [see *Cullen*, 1991, and references therein]), it is, more generally, widely admitted that oligotrophic waters are dominated by picoplanktonic cells, while large cells, such as diatoms, would be typical of eutrophic waters [e.g., *Yentsch and Phinney*, 1989]. The second argument is related to the vertical distribution of algae: the hypothesis that deep chlorophyll maximum (DCM) in oligotrophic waters would mostly result from increased intracellular pigment concentration, rather than from increased cell number density, has been supported by many observations [e.g., *Kiefer et al.*, 1976; *Beers et al.*, 1982; *Kitchen and Zaneveld*, 1990]. Although this is probably not an ubiquitous rule, as various mechanisms have been invoked for the DCM formation (see discussion by *Cullen* [1982]), these observations suggest that there may exist a correlation between c_i and ⟨chl⟩ along the vertical. The actual, and likely important, fluctuations in the ⟨chl⟩–c_id relationship, however, are presumably the most important cause of scatter in the observed relationship between Q^*_a and ⟨chl⟩.

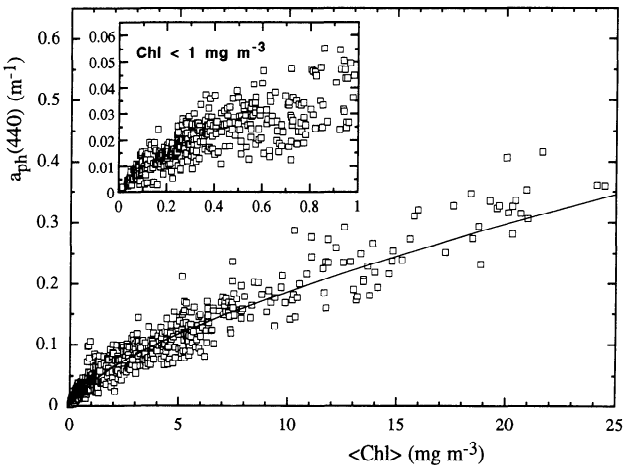

Figure 4. Variations of the absorption coefficient of phytoplankton at 440 nm $a_{ph}(440)$ (in m^{-1}), as a function of the (chl a + divchl a) concentration, for the same set of data as in Figure 1. An enlargement of the area corresponding to concentrations lower than 1 mg m^{-3} is shown in inset. The curve obtained by least squares fit ($a_{ph}(440)$ = 0.0403 ⟨chl⟩$^{0.668}$) is displayed as a solid line.

4.2. The Effect of Pigment Composition

This effect has been examined by considering the data from Eumeli and Tomofront cruises, for which detailed HPLC pigment information was available. It has been ob-

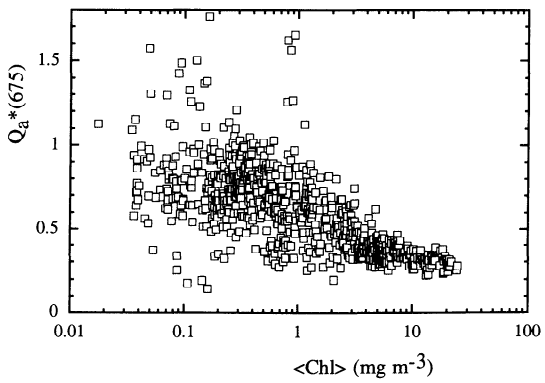

Figure 5. Variations of the dimensionless factor $Q^*_a(675)$ (see (2)), as a function of the (chl a + divchl a) concentration ⟨chl⟩ (in milligrams per cubic meter), for the same data set as in Figure 1.

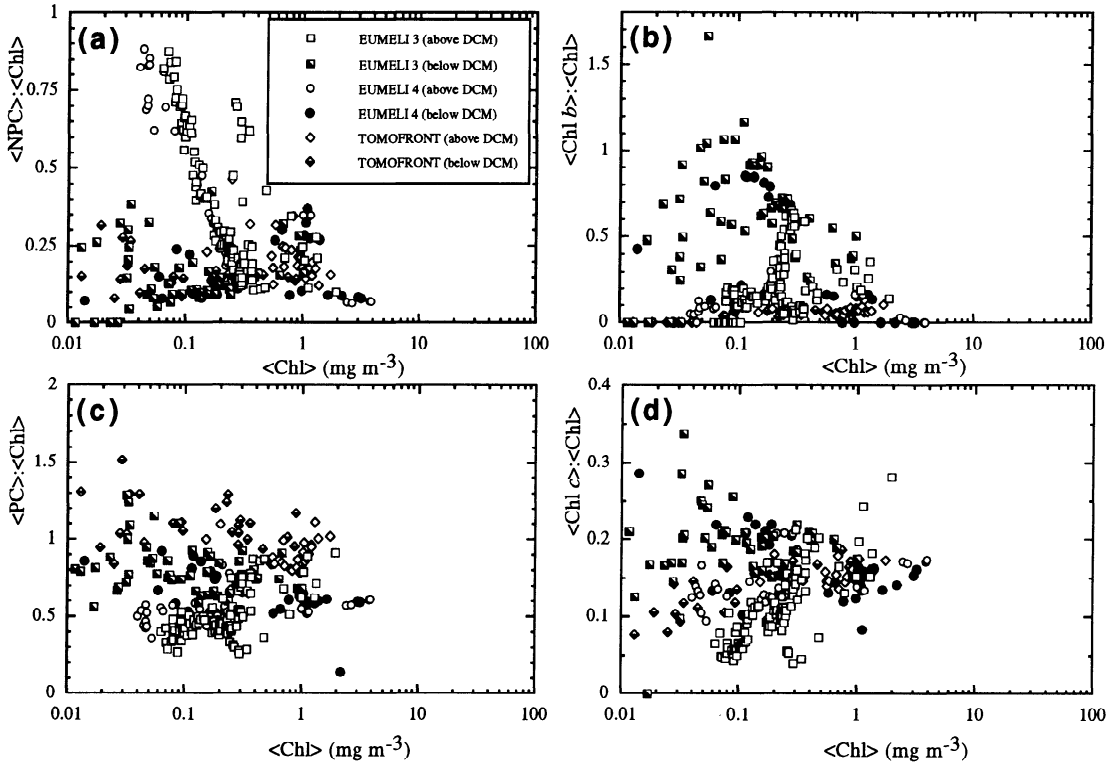

Figure 6. (a) Variations of the ratio of nonphotosynthetic carotenoids-to-(chl *a* + divchl *a*) concentrations, ⟨NPC⟩/⟨chl⟩, as a function of ⟨chl⟩ (in milligrams per cubic meter), for the Eumeli 3 and 4 and Tomofront cruises. Nonphotosynthetic carotenoids include zeaxanthin, alloxanthin, β-carotene, diadinoxanthin, and diatoxanthin. (b) Variations of the ratio of (chl *b* + divchl *b*)-to-(chl *a* + divchl *a*) concentrations, ⟨chl b⟩/⟨chl⟩, as a function of ⟨chl⟩, for the same cruises. (c) Variations of the ratio of photosynthetic carotenoids-to-(chl *a* + divchl *a*) concentrations, ⟨PC⟩/⟨chl⟩, as a function of ⟨chl⟩, for the same cruises. Photosynthetic carotenoids include fucoxanthin, peridinin, 19′-HF, 19′-BF, prasinoxanthin, and α-carotene. (d) Variations of the ratio of (chl c_1 + chl c_2 + chl c_3)-to-(chl *a* + divchl *a*) concentrations, ⟨chl *c*⟩/⟨chl⟩, as a function of ⟨chl⟩, for the same cruises.

served that in oligotrophic waters the concentration ratio of nonphotosynthetic (mainly photoprotective) carotenoids (NPC) to ⟨chl⟩ (⟨NPC⟩/⟨chl⟩) was continuously decreasing from the surface to deep waters. As a result, the relative concentration of these pigments varies along the vertical inversely to ⟨chl⟩, at least between the surface and the DCM (see Figure 6a, open symbols). Furthermore, the relative concentration of these pigments is, on average, higher in oligotrophic than in mesotrophic waters. This favors the increase of a^*_{ph} in the blue part of the spectrum with decreasing ⟨chl⟩, as the absorption bands of the nonphotosynthetic pigments cover the 400- to 530-nm domain, with main maxima around 460 and 490 nm (see, e.g., *Bidigare et al.* [1990]). The inverse covariation between ⟨NPC⟩ and ⟨chl⟩, however, disappears below the DCM, where both groups of pigments decrease along the vertical.

The (chl *b* plus divchl *b*)/⟨chl⟩ ratio, conversely, tends to increase from the surface down to the DCM, which impairs the inverse relationship between a^*_{ph} and ⟨chl⟩ (Figure 6b, open symbols). Below the DCM, this ratio remains steadily high (Figure 6b, solid symbols), and the corresponding samples are characterized by low ⟨chl⟩–high a^*_{ph} values, within the absorption bands of chl *b* and divinyl chl *b* (400–500 and 630–670 nm, with maxima around 470 and 650 nm). They contribute therefore to the inverse relationship between ⟨chl⟩ and a^*_{ph} in these wavelength domains.

The effects of other accessory pigments (mainly photosynthetic carotenoids and chl *c*) on a^*_{ph} are still more complex, as their relative abundances with respect to ⟨chl⟩ show no clear tendency (Figures 6c and 6d). Therefore the scatter observed in the a^*_{ph}–⟨chl⟩ relationship, especially in oligotrophic waters (Figure 1), is believed to mainly originate from these fluctuations in pigment composition, at least for what concerns the blue part of the spectrum.

In summary, the relative abundances of accessory pigments remain, in spite of their fluctuations, consistently high in oligotrophic waters compared with mesotrophic or eutrophic waters (mainly because of the presence of nonphotosynthetic pigments in the surface layer and of chl *b*-like pigments in the deeper layer). It can be concluded that variations in pigment composition contribute significantly to the a^*_{ph}–⟨chl⟩ relationship. This is also attested to by the shape of the $B(\lambda)$ spectrum (Figure 3), which exhibits maxima around 480 nm and 650 nm, in relation to the high concentration of nonphotosynthetic carotenoids, chl *b*, and divinyl chl *b* in oligotrophic waters compared with chlorophyll-rich waters. The additional small band located around 600 nm on the $B(\lambda)$ spectrum has also been observed on absorption spectra of *Prochlorococcus* [*Partensky et al.*, 1993], a species mainly present in oligotrophic waters.

4.3. Can the Relative Contributions of the Package Effect and the Pigment Composition to a^*_{ph} Variations Be Assessed?

Knowing the variations in the concentrations of the various pigments (relative to ⟨chl⟩) and their specific absorption coefficients, it would be possible, in the absence of package effect, to estimate the associate variations in a^*_{ph} at a given wavelength. Therefore the contribution of accessory pigments to the a^*_{ph}–⟨chl⟩ relationship could, in principle, be assessed. Such an estimate, however, is not possible, because the relationship between the absorption coefficient of cellular matter a_{cm} (as modified by the presence of accessory pigments) and a^*_{ph} is nonlinear (see (2)–(4)), and any change in a_{cm} reacts on the amplitude of the package effect.

In summary, it can be stated that the package effect induces a threefold reduction of the height of the red absorption band when ⟨chl⟩ increases from 0.02 to 25 mg m^{-3}; therefore, in the blue part of the spectrum (where a^*_{ph} varies about tenfold), this effect is certainly responsible for part of the covariation between a^*_{ph} and ⟨chl⟩. The relative contributions of the package effect and of accessory pigments, however, are intermingled and cannot be simply partitioned in this wavelength domain.

5. Application: Parameterization of the Chlorophyll-Specific Absorption Spectra of Phytoplankton

Equation (1), with the A and B values provided in Table 2, can be used to produce "mean" a^*_{ph} spectra as a function of the chlorophyll concentration in the medium. They are displayed in Figure 7a, for ⟨chl⟩ ranging from 0.03 to 10 mg m^{-3}; the changes in shape of the a^*_{ph} spectra are evidenced by a normalization at 440 nm in Figure 7b. This parameterization predicts a variation of $a^*_{ph}(440)$ by approximately a factor of 10 when ⟨chl⟩ varies over 3 orders of magnitude (0.02 to 20 mg m^{-3}). This range of variation is narrower than that predicted by *Carder et al.* [1991] (0.12 to 0.008 m^2 mg^{-1} for chl *a* concentrations varying from 0.01 to 10 mg m^{-3}). It is, conversely, larger than that shown by the typical absorption curves proposed by *Wozniak et al.* [1992], with $a^*_{ph}(440)$ decreasing from 0.22 to 0.04 m^2 mg^{-1} over the ⟨chl⟩ range 0.02–20 mg m^{-3}.

The present parameterization reproduces properly the "flattening" of absorption spectra with increasing ⟨chl⟩ (Figure 7a), resulting both from the package effect [see *Morel and Bricaud*, 1981, Figure 2] and from the decrease in the relative concentrations of accessory pigments. Consistently with the $B(\lambda)$ spectrum, the enhanced absorption in the domain 440–490 nm for oligotrophic waters is also reproduced (Figure 7b). For $\lambda > 495$ nm, beyond the hinge point of all normalized spectra, the situation is inverted, and absorption in the green and red parts of the spectrum decreases, relative to that at 440 nm, with decreasing ⟨chl⟩ (Figure 7c). The ratio $a^*_{ph}(675)/a^*_{ph}(440)$, for instance, decreases by a factor of 3 when ⟨chl⟩ decreases from 10 to 0.03 mg m^{-3} (Figure 7c). Note that from eutrophic to oligotrophic waters, the blue maximum is progressively shifted from 435–440 to 446 nm. It has already been observed that in very oligotrophic waters the blue maximum is shifted by 6–8 nm toward longer wavelengths, in correspondence with the shift of the in vivo absorption maximum of divinyl chl *a* (~447 nm), compared with that of chl *a* (~440 nm) [*Bricaud and Stramski*, 1990]. Note, also, that at high ⟨chl⟩ values a large shoulder appears in the vicinity of 530 to 550 nm. This feature, to be considered with caution, very likely originates from a peculiarity of our data set, in which some samples from mesotrophic waters are characterized by a

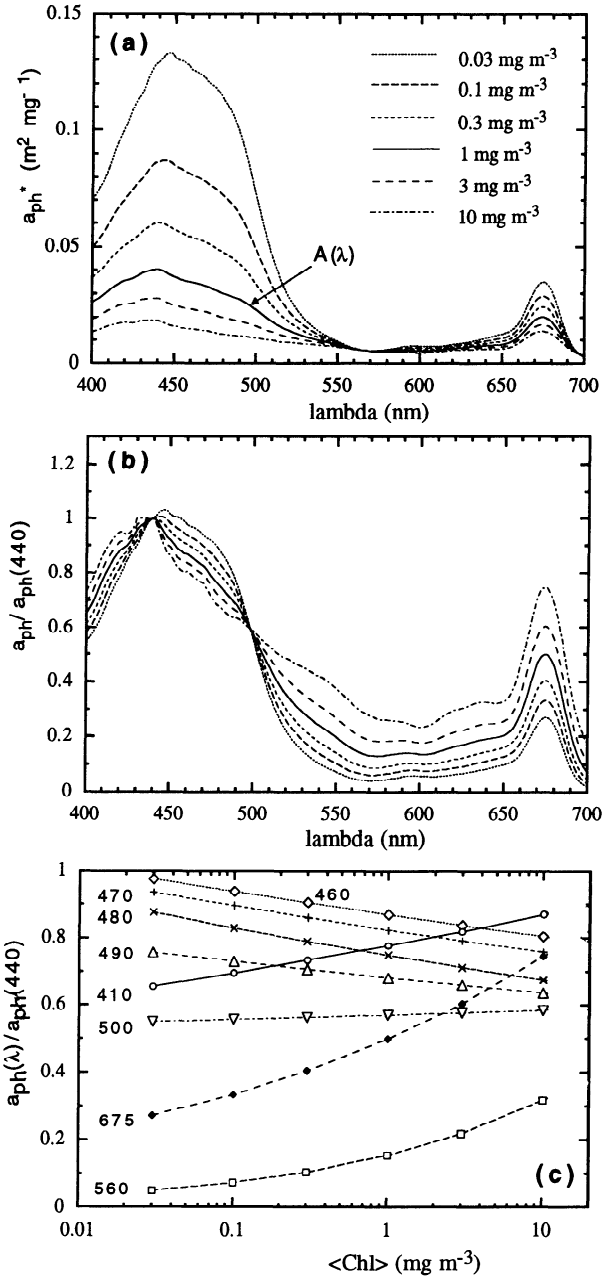

Figure 7. (a) Chlorophyll-specific absorption spectra of living phytoplankton $a^*_{ph}(\lambda)$ for various values of the (chl *a* + divchl *a*) concentration ⟨chl⟩ (0.03 to 10 mg m^{-3}), as reconstructed from (1), with the spectral values of A and B listed in Table 2. Note that the $A(\lambda)$ values are shown as the absorption spectrum when ⟨chl⟩ = 1 mg m^{-3}. (b) Same as Figure 7a, with the a^*_{ph} spectra normalized at 440 nm. (c) Variations of absorption ratios, $a^*_{ph}(\lambda)/a^*_{ph}(440)$, derived from the reconstructed absorption spectra for various wavelengths as functions of the (chl *a* + divchl *a*) concentration.

high concentration of phycoerythrin-containing cyanobacteria (Eumeli 3 and 4 cruises).

6. Conclusions

The evolution of the chlorophyll-specific absorption coefficient of phytoplankton $a^*_{ph}(\lambda)$ with the chl a concentration, as analyzed and quantified in this paper, merges typical variations in both package effect and pigment composition in various oceanic waters. The proposed parameterization is obviously not applicable outside the chlorophyll range corresponding to the data body, nor can it be used on a sample-to-sample basis. Therefore it is not aimed at prompting the bio-opticists to abandon $a^*_{ph}(\lambda)$ measurements and replace them with absorption spectra computed from the ⟨chl⟩ level. Simultaneous measurements of a^*_{ph} spectra and light-photosynthesis curves, in particular, definitely remain a prerequisite to accurate determinations of the maximum quantum yield for growth of phytoplanktonic populations.

More generally, this parameterization does not pretend to be applicable to all situations, as it has been derived from data collected in only six regions of the world ocean. To our knowledge, however, this data set is presently the largest one available for studying the natural variations of $a^*_{ph}(\lambda)$. The construction of larger data banks in the near future should contribute to improving this knowledge.

Such a parameterization, if confirmed by further data, could provide substantial improvements to the estimate of large-scale variations of $a^*_{ph}(\lambda)$, when measurements are not feasible or available. This is the case, for instance, when converting satellite pigment concentration maps into primary production maps by operating "physiological" models. While $a^*_{ph}(\lambda)$ has frequently been assumed as constant in such models, the present study predicts a variation of $a^*_{ph}(440)$ by about a factor of 10 when the chl a concentration varies over 3 orders of magnitude (0.02–20 mg m^{-3}), a realistic range for the world ocean.

In principle, as the instantaneous carbon fixation rate is (nonlinearly) related to the light absorption capacity of living cells, the impact of using chlorophyll-dependent a^*_{ph} spectra, instead of constant coefficients, upon primary production computations can be evaluated. The actual error, however, is not easily predictable, because of the impact of another input parameter, the maximum quantum yield for carbon fixation Φ_{max}. There is some evidence that Φ_{max} is also very variable and possibly positively correlated with nutrient availability [see *Falkowski et al.*, 1992, and references therein]. Therefore its variations with the trophic state of waters could partially compensate those of absorption. The amplitude of its actual variations in the world ocean, however, is still very poorly documented, so that the final impact upon the estimates of carbon fixation rate is unknown. Improvement in primary production modeling at global or regional scales is therefore still pending on the availability of a large data bank including simultaneous measurements of living phytoplankton absorption coefficients and light-photosynthesis curves.

Appendix

In spite of mathematical appearance, analysis of the variations of $a^*_{ph}(\lambda)$ [$=a_{ph}(\lambda)/\langle\text{chl}\rangle$] as a function of ⟨chl⟩ is allowed. In contrast to $a_{ph}(\lambda)$, $a^*_{ph}(\lambda)$, which represents the absorption cross section of phytoplankton per mass unit of chlorophyll a, is a variable independent of ⟨chl⟩, the chlorophyll a concentration in the medium, and only dependent on the algal cell size and intracellular pigment concentration [see *Morel and Bricaud*, 1981, equation (5)]. Numerical results strictly identical to those presented in this paper are obtained as well by studying the curvature of the relationship between $a_{ph}(\lambda)$ and ⟨chl⟩; an example is given in Figure 4 for $a_{ph}(440)$ (see also Table 2).

A possible artifact in the application of (1) (see text) to $a^*_{ph}(\lambda)$ and ⟨chl⟩, however, may originate from the random error made on the ⟨chl⟩ determinations err_C. As actually applied, (1) can be rewritten as

$$\frac{a_{ph}(\lambda)\ \text{err}_a}{\langle\text{chl}\rangle\ \text{err}_C} = a^*_{ph}(\lambda)\ \frac{\text{err}_a}{\text{err}_C} = f(\langle\text{chl}\rangle\ \text{err}_C)$$

where err_a and err_C represent the relative random errors made on $a_{ph}(\lambda)$ and ⟨chl⟩ determinations, respectively. Relative to (1), the above equation involves a bias produced by the appearance of err_C on both sides of the equation, which leads to a reciprocal dependency. To assess the extent of this bias, we generated 5000 ⟨chl⟩ values logarithmically ranging from 0.02 to 50 mg m^{-3} and err_C random values between 0.5 and 1.5 (±50% error on ⟨chl⟩ determination); err_a was taken to be equal to 1. First, assuming $a^*_{ph}(\lambda)$ to be constant, no significant relationship could be found between $(a^*_{ph}(\lambda)/\text{err}_C)$ and $(\langle\text{chl}\rangle\ \text{err}_C)$. This result shows that if no relationship basically existed between $a^*_{ph}(\lambda)$ and ⟨chl⟩, the introduction of a random error in (1) could not produce an artifactual one. Second, if we express $a^*_{ph}(\lambda)$ as

$$a^*_{ph}(\lambda) = 0.0403\ \langle\text{chl}\rangle^{-0.332}$$

in agreement with the power function found in this study at 440 nm (see Table 2), the A and B values obtained from the least squares fit of a power function to $(a^*_{ph}(\lambda)/\text{err}_C)$ as a function of $(\langle\text{chl}\rangle\ \text{err}_C)$ differ by less than 3% from those in the above equation. This result demonstrates that the relationships between $a^*_{ph}(\lambda)$ and ⟨chl⟩ presented in the present study are not significantly biased by experimental errors on ⟨chl⟩. Both these results can be explained by the large range of variation in ⟨chl⟩ (3 orders of magnitude) compared with the one expected (at worst) for err_C.

Notation

λ	wavelength, nm.
⟨chl⟩	chlorophyll a concentration (including divinyl chl a), mg m^{-3}.
⟨NPC⟩	concentration of nonphotosynthetic carotenoids, mg m^{-3}.
⟨PC⟩	concentration of photosynthetic carotenoids, mg m^{-3}.
a	absorption coefficient of the water body, m^{-1}.
b_b	backscattering coefficient of the water body, m^{-1}.
R	diffuse reflectance.
F	proportionality factor between R and b_b/a.
a_p	absorption coefficient of particles, m^{-1}.
a_d	absorption coefficient of nonalgal material, m^{-1}.
a_{ph}	absorption coefficient of phytoplankton, m^{-1}.
a^*_p	chl a-specific absorption coefficient of particles, m^2 mg^{-1}.

a^*_{ph} chl a-specific absorption coefficient of phytoplankton, $m^2\ mg^{-1}$.
A, B numerical constants in the relationship between a^*_{ph} and ⟨chl⟩ (equation (1)).
z depth, m.
z_e euphotic depth, m.
K_d diffuse attenuation coefficient for downwelling irradiance, m^{-1}.
k_c chl a-specific diffuse attenuation coefficient for downwelling irradiance, $m^2\ mg^{-1}$.
a^*_{sol} chl a-specific absorption coefficient of cellular matter (hypothetically dispersed into solution), $m^2\ mg^{-1}$.
Q_a efficiency factor for absorption by phytoplankton.
Q^*_a package effect index (defined in (2)).
ρ' optical thickness of a cell corresponding to absorption along a diameter (defined in (4)).
a_{cm} absorption coefficient of cellular matter, m^{-1}.
d cell size, μm.
β path length amplification by a glass-fiber filter.
Φ_{max} maximum quantum yield for carbon fixation, mol C (mol quanta)$^{-1}$.
err_C relative random error on chlorophyll determination.
err_a relative random error on a_{ph} determination.

Acknowledgments. This study was supported by Centre National de la Recherche Scientifique (UA 353 and GDR 869) and by various agencies through the JGOFS-FRANCE ("Eumeli" and "Frontal") programs. Data from the St. Lawrence estuary and Gulf were acquired within the programs of the Maurice Lamontagne Institute (Department of Fisheries and Oceans, Biological Oceanography Division) and GIROQ (Groupe interuniversitaire de recherches océanographiques du Québec). The authors wish to thank the chief scientists and crews of the different cruises during which the data used in this work have been collected. J. Neveux is duly acknowledged for making available results of spectrofluorometric measurements of pigment concentrations, D. Stramski for allowing use of Chlomax data, J. Campbell for suggesting Figure 4, S. Sathyendranath for helpful comments, and D. A. Phinney and two anonymous referees for thorough criticism of the manuscript.

References

Anderson, T. R., A spectrally averaged model of light penetration and photosynthesis, *Limnol. Oceanogr., 38*, 1403–1419, 1993.

Babin, M., J. C. Therriault, L. Legendre, and A. Condal, Variations in the specific absorption coefficient for natural phytoplankton assemblages: Impact on estimates of primary production, *Limnol. Oceanogr., 38*, 154–177, 1993.

Babin, M., J. C. Therriault, L. Legendre, B. Nicke, R. Reuter, and A. Condal, Relationship at sea between the maximum quantum yield of carbon fixation and the minimum quantum yield of chlorophyll *a* fluorescence, *Limnol. Oceanogr.*, in press, 1995.

Beers, J. R., F. M. H. Reid, and G. L. Steward, Seasonal abundance of the microplankton population in the North Pacific central gyre, *Deep Sea Res., Part A, 29*, 227–245, 1982.

Bidigare, R. R., M. E. Ondrusek, J. H. Morrow, and D. A. Kiefer, *In vivo* absorption properties of algal pigments, Ocean Optics 10, *Proc. SPIE Int. Soc. Opt. Eng., 1302*, 290–302, 1990.

Bricaud, A., and D. Stramski, Spectral absorption coefficients of living phytoplankton and nonalgal biogenous matter: A comparison between the Peru upwelling area and Sargasso Sea, *Limnol. Oceanogr., 35*, 562–582, 1990.

Bricaud, A., A. Morel, and L. Prieur, Optical efficiency factors of some phytoplankters, *Limnol. Oceanogr., 28*, 816–832, 1983.

Carder, K. L., R. G. Steward, J. H. Paul, and G. A. Vargo, Relationships between chlorophyll and ocean color constituents as they affect remote-sensing reflectance models, *Limnol. Oceanogr., 31*, 403–413, 1986.

Carder, K. L., S. K. Hawes, K. A. Baker, R. C. Smith, R. G. Steward, and B. G. Mitchell, Reflectance model for quantifying chlorophyll *a* in the presence of productivity degradation products, *J. Geophys. Res., 96*(C11), 20,599–20,611, 1991.

Claustre, H., and J. C. Marty, Specific phytoplankton biomasses and their relation to primary production in the tropical North Atlantic, *Deep Sea Res., Part I*, in press, 1995.

Cullen, J. J., The deep chlorophyll maximum: Comparing vertical profiles of chlorophyll a, *Can. J. Fish. Aquat. Sci., 39*, 791–803, 1982.

Cullen, J. J., Hypotheses to explain high-nutrient conditions in the open sea, *Limnol. Oceanogr., 36*, 1578–1599, 1991.

Falkowski, P. G., R. M. Greene, and R. J. Geider, Physiological limitations on phytoplankton productivity in the ocean, *Oceanography, 5*(2), 84–91, 1992.

Gordon, H. R., Dependence of the diffuse reflectance of natural waters on the sun angle, *Limnol. Oceanogr., 34*, 1484–1489, 1989.

Groupe MEDIPROD, Campagne PACIPROD, *Campagnes Océanogr. Fr. 7*, Inst. Fr. de Rech. pour l'Explor. de la Mer, Brest, France, 1989.

Groupe MEDIPROD, Campagne MEDIPROD VI, *Campagnes Océanogr. Fr. 16*, Inst. Fr. de Rech. pour l'Explor. de la Mer, Brest, France, 1991.

Groupe MEDIPROD, Campagne CHLOMAX, *Campagnes Océanogr. Fr. 17*, Inst. Fr. de Rech. pour l'Explor. de la Mer, Brest, France, 1992.

Herbland, A., A. Le Bouteiller and P. Raimbault, Size structure of phytoplankton biomass in the equatorial Atlantic ocean, *Deep Sea Res., Part A, 32*, 819–836, 1985.

Hoepffner, N., and S. Sathyendranath, Bio-optical characteristics of coastal waters: Absorption spectra of phytoplankton and pigment distribution in the western North Atlantic, *Limnol. Oceanogr., 37*, 1660–1679, 1992.

Holm-Hansen, O., and B. Riemann, Chlorophyll a determination: Improvements in methodology, *Oikos, 30*, 438–447, 1978.

Kiefer, D. A., and B. G. Mitchell, A simple, steady-state description of phytoplankton growth based on absorption cross-section and quantum efficiency, *Limnol. Oceanogr., 28*, 770–776, 1983.

Kiefer, D. A., R. J. Olson, and O. Holm-Hansen, Another look at the nitrate and chlorophyll maxima in the central North Pacific, *Deep Sea Res., 23*, 1199–1208, 1976.

Kirk, J. T. O., A theoretical analysis of the contribution of algal cells to the attenuation of light within waters, II, Spherical cells, *New Phytol., 75*, 21–36, 1975.

Kirk, J. T. O., Dependence of relationship between inherent and apparent optical properties of water on solar altitude, *Limnol. Oceanogr., 29*, 350–356, 1984.

Kishino, M., M. Takahashi, N. Okami, and S. Ichimura, Estimation of the spectral absorption coefficients of phytoplankton in the sea, *Bull. Mar. Sci., 37*, 634–642, 1985.

Kitchen, J. C., and J. R. V. Zaneveld, On the noncorrelation of the vertical structure of light scattering and chlorophyll a in case I waters, *J. Geophys. Res., 95*(C11), 20,237–20,246, 1990.

Mitchell, B. G., and O. Holm-Hansen, Bio-optical properties of Antarctic Peninsula waters: Differentiation from temperate ocean models, *Deep Sea Res., Part A, 38*, 1009–1028, 1991.

Mitchell, B. G., and D. A. Kiefer, Chlorophyll *a*-specific absorption and fluorescence excitation spectra for light-limited phytoplankton, *Deep Sea Res., Part A, 35*, 639–663, 1988a.

Mitchell, B. G., and D. A. Kiefer, Variability in pigment specific particulate fluorescence and absorption spectra in the northeastern Pacific Ocean, *Deep Sea Res., Part A, 35*, 665–689, 1988b.

Morel, A., Optical modeling of the upper ocean in relation to its biogenous matter content (case I waters), *J. Geophys. Res., 93*(C9) 10,749–10,768, 1988.

Morel, A., Light and marine photosynthesis: A spectral model with geochemical and climatological implications, *Prog. Oceanogr., 26*, 263–306, 1991.

Morel, A., and J. M. André, Pigment distribution and primary production in the western Mediterranean as derived and modeled from coastal zone color scanner observations, *J. Geophys. Res., 96*(C7), 12,685–12,698, 1991.

Morel, A., and A. Bricaud, Theoretical results concerning light absorption in a discrete medium, and application to specific absorption of phytoplankton, *Deep Sea Res., Part A, 28*, 1375–1393, 1981.

Morel, A., and B. Gentili, Diffuse reflectance of oceanic waters: Its dependence on sun angle as influenced by the molecular scattering contribution, *Appl. Opt.*, *30*, 4427–4438, 1991.

Neveux, J., and F. Lantoine, Spectrofluorometric assay of chlorophylls and pheopigments using least square approximation technique, *Deep Sea Res., Part I*, *40*, 1747–1765, 1993.

Parsons, T. R., Y. Maita, and C. M. Lalli, *A Manual of Chemical and Biological Methods for Seawater Analysis*, 173 pp., Pergamon, New York, 1984.

Partensky, F., N. Hoepffner, W. K. W. Li, O. Ulloa, and D. Vaulot, Photoacclimation of *Prochlorococcus* sp. (Prochlorophyta) strains isolated from the North Atlantic and the Mediterranean Sea, *Plant Physiol.*, *101*, 285–296, 1993.

Platt, T., and S. Sathyendranath, Oceanic primary production: Estimation by remote sensing at local and regional scales, *Science*, *241*, 1613–1620, 1988.

Prieur, L., and A. Morel, Relations théoriques entre le facteur de réflexion diffuse de l'eau de mer, à diverses profondeurs, et les caractéristiques optiques, paper presented at 16th General Assembly, Int. Union of Geod. and Geophys., Grenoble, France, Aug. 25 to Sept. 6, 1975.

Prieur, L., and S. Sathyendranath, An optical classification of coastal and oceanic waters based on the specific spectral absorption curves of phytoplankton pigments, dissolved organic matter, and other particulate materials, *Limnol. Oceanogr.*, *26*, 671–689, 1981.

Smith, R. C., and K. S. Baker, Optical classification of natural waters, *Limnol. Oceanogr.*, *23*, 260–267, 1978.

Trüper, H. G., and C. S. Yentsch, Use of glass-fiber filters for the rapid preparation of in vivo absorption spectra of photosynthetic bacteria, *J. Bacteriol.*, *94*, 1255–1256, 1967.

van de Hulst, H. C., *Light Scattering by Small Particles*, John Wiley, New York, 1957.

Wozniak, B., and M. Ostrowska, Optical absorption properties of phytoplankton in various seas, *Oceanologia*, *29*, 117–146, 1990.

Wozniak, B., J. Dera, and O. Koblentz-Mischke, Modeling the relationship between primary production, optical properties and nutrients in the sea (as a basis for indirectly estimating primary production), Ocean Optics 11, Proc. *SPIE Int. Soc. Opt. Eng.*, *1750*, 246–275, 1992.

Yentsch, C. S., and D. W. Menzel, A method for the determination of phytoplankton chlorophyll and pheophytin by fluorescence, *Deep Sea Res.*, *10*, 221–231, 1963.

Yentsch, C. S., and D. A. Phinney, A bridge between ocean optics and microbial ecology, *Limnol. Oceanogr.*, *34*, 1694–1705, 1989.

M. Babin, A. Bricaud, H. Claustre, and A. Morel, Laboratoire de Physique et Chimie Marines, CNRS and Université Pierre et Marie Curie, BP 8, F-062320 Villefranche-sur-Mer, France.

(Received April 7, 1994; revised October 18, 1994; accepted December 22, 1994.)